EMBO reports

scientific report

Structure and function of BamE within the outer membrane and the β-barrel assembly machine

Timothy J. Knowles[1], Douglas F. Browning[2]*, Mark Jeeves[1], Riyaz Maderbocus[1], Sandya Rajesh[1], Pooja Sridhar[1], Eleni Manoli[1], Danielle Emery[2], Ulf Sommer[3], Ashley Spencer[2], Denisse L. Leyton[2], Derrick Squire[2], Roy R. Chaudhuri[2], Mark R. Viant[3], Adam F. Cunningham[2], Ian R. Henderson[2+] & Michael Overduin[1]*

[1]School of Cancer Sciences, [2]School of Immunity and Infection, and [3]School of Biosciences, University of Birmingham, Birmingham, UK

Insertion of folded proteins into the outer membrane of Gram-negative bacteria is mediated by the essential β-barrel assembly machine (Bam). Here, we report the native structure and mechanism of a core component of this complex, BamE, and show that it is exclusively monomeric in its native environment of the periplasm, but is able to adopt a distinct dimeric conformation in the cytoplasm. BamE is shown to bind specifically to phosphatidylglycerol, and comprehensive mutagenesis and interaction studies have mapped key determinants for complex binding, outer membrane integrity and cell viability, as well as revealing the role of BamE within the Bam complex.

Keywords: Bam complex; BamE; Omp85; outer membrane biogenesis; SmpA

EMBO *reports* (2011) **12**, 123–128. doi:10.1038/embor.2010.202

INTRODUCTION

The outer membrane of Gram-negative bacteria is a selective barrier essential for protection against environmental factors and mediating the flow of essential metabolites. The outer membrane has peripheral and integral membrane proteins and contains specific phospholipids including phosphatidylglycerol, while its outer leaflet is enriched with lipopolysaccharide. The outer membrane protein (OMP) family are integral membrane proteins associated with basic physiological functions, virulence and multi-drug resistance, and hence have fundamental roles in maintaining cellular viability (Bos *et al*, 2007). The majority of OMPs adopt a β-barrel conformation and require the barrel assembly machine (Bam) complex to be efficiently inserted into the outer membrane as a folded species (Bos *et al*, 2007; Knowles *et al*, 2008, 2009b). In *Escherichia coli*, this complex consists of five Bam proteins, designated A–E. BamA is an essential integral OMP, whereas BamB–E are peripheral lipoproteins of which only BamD is essential (Voulhoux *et al*, 2003; Wu *et al*, 2005; Sklar *et al*, 2007). Loss of BamB, BamC or BamE results in membrane barrier defects manifesting as hypersensitivity to small toxic molecules including vancomycin and sodium dodecyl sulphate (SDS; Ruiz *et al*, 2005; Sklar *et al*, 2007). Previous studies have revealed that BamD interacts directly with BamA and functions as a scaffold for BamC and BamE, whereas BamB independently interacts with BamA (Malinverni *et al*, 2006; Kim *et al*, 2007; Sklar *et al*, 2007; Vuong *et al*, 2008). Recently, these subcomplexes have been reconstituted, showing that some or all of BamCDE is required for function (Hagan *et al*, 2010). These data, together with the fact that α-proteobacteria such as *Brucella* only have a complex of BamADE (Gatsos *et al*, 2008), suggest that BamE, although not essential, has a key role in the Bam complex.

Here, we report the solution structure of the native periplasmic state of *E. coli* BamE. This structure is one of two forms that BamE is able to adopt, but it is the only state that accumulates within the periplasmic space. Scanning mutagenesis and interaction mapping have revealed sites required for localization to the Bam complex, as well as phosphatidylglycerol recognition and maintenance of outer membrane integrity and cell viability.

RESULTS AND DISCUSSION

To ensure a natural folding environment, BamE was expressed in the *E. coli* periplasm using a PelB signal sequence (MKYLLP TAAAGLLLLAANPAMA) and with a C20S mutation to prevent amino-terminal acylation. Periplasmic release by osmotic shock yielded a protein that was natively processed and monomeric, as confirmed by N-terminal sequencing, SDS–polyacrylamide gel electrophoresis, gel filtration and analytical ultracentrifugation (supplementary Fig S1A online). By contrast, whole-cell purification yielded a mixture of monomer and dimer (supplementary Fig S1B online). Both species were stable, although their NMR spectra were not superimposable (supplementary Fig S1E,F online). The different folding outcomes are dictated by the environment; expression at lower temperatures favours periplasmic monomer and at elevated temperatures yields uncleaved

[1]School of Cancer Sciences, [2]School of Immunity and Infection, and [3]School of Biosciences, University of Birmingham, Edgbaston, Birmingham B15 2TT, UK
*These authors contributed equally to this work
[+]Corresponding author. Tel: +44 121 414 3802; Fax: +44 121 414 4486; E-mail: i.r.henderson@bham.ac.uk

Received 31 May 2010; revised 16 November 2010; accepted 16 November 2010; published online 7 January 2011

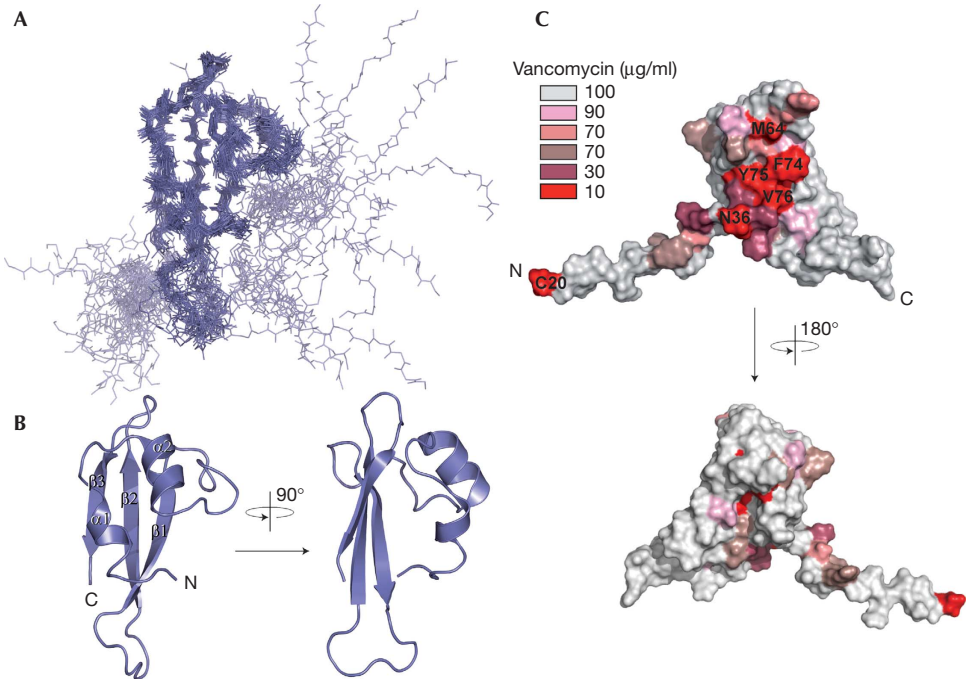

Fig 1 | BamE solution structure. (**A**) Backbone model of the 20 lowest-energy structures. Secondary structural elements: α-helices, residues 40–45 and 52–58; β-strands, residues 72–78, 88–95 and 100–106. (**B**) Ribbon diagram of the structure (residues 36–108) closest to the mean, coloured according to **A**. (**C**) Surface representation showing the positions of residues that on glycine substitution altered the minimal inhibitory concentration of vancomycin. Different levels of susceptibility were observed depending on mutation and are highlighted accordingly. BamE, β-barrel assembly machine E.

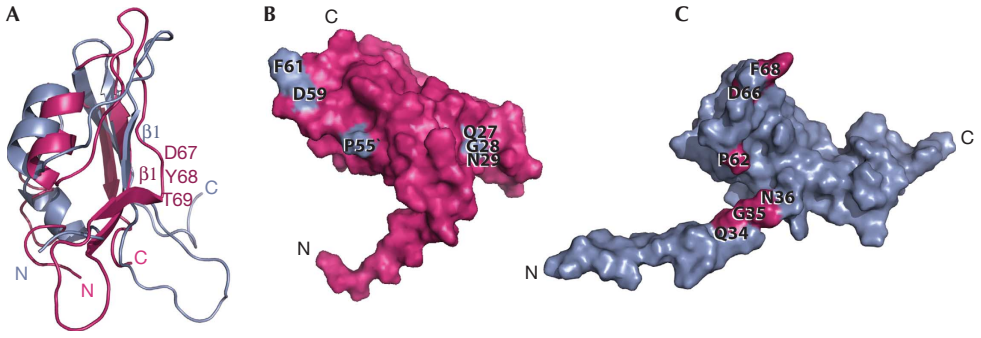

Fig 2 | Structural comparison. (**A**) Ribbon diagrams of the DaliLite (Holm & Park, 2000) fit of *Escherichia coli* BamE (grey) to *Xanthomonas axonopodis* pv. *citri* BamE (pink; Protein Data Bank number 2pxg; Vanini *et al*, 2008). An alignment of this fit can be seen in supplementary Fig S2 online. Residues 67–69 of *X. axonopodis* pv. *citri* BamE are labelled and form a β1-strand kink not present in the *E. coli* protein. (**B**) Surface representation of *X. axonopodis* pv. *citri* BamE showing the positions of the QGN motif and the highly conserved Pro 55, Asp 59 and Phe 61 (shown in grey). (**C**) Similar view of *E. coli* BamE showing the positions of the homologous residues in pink and highlighting the distinct position of the QGN motif. BamE, β-barrel assembly machine E.

cytosolic dimer (supplementary Fig S1C,D online). Analysis of expression levels showed that increasing the temperature prevents export from the cytosol, suggesting that the dimer is a misfolded aggregate. As the native environment for BamE is the periplasm, only the monomer was prepared for structural elucidation.

The structure of full-length mature *E. coli* BamE (C20S mutation) was determined by NMR spectroscopy, yielding an ensemble with a backbone RMSD of 0.83 Å for the structured domain (supplementary Table S1 online). The fold consists of an anti-parallel β-sheet packed against a pair of α-helices with an ααβββ topology (Fig 1A,B). The N-terminal acylation site connects through an unstructured 20-residue linker. The most similar known structure is that of the orthologous *Xanthomonas axonopodis* protein, with which it shares 23% sequence identity (Vanini *et al*, 2008). However, the structures differ, particularly in the β1-strand and conserved QGN elements, with a backbone RMSD of 3.2 Å (Fig 2; supplementary Fig S2 online).

The functionally relevant BamE residues required for outer membrane barrier function were revealed by comprehensive mutagenesis and functional analyses. Wild-type *E. coli* can be

discriminated from *E. coli* Δ*bamE* by the inability of the latter to grow in the presence of vancomycin (Ruiz *et al*, 2005; Sklar *et al*, 2007), which is a standard assay for outer membrane integrity. Biolog screening confirmed that vancomycin was one of the most effective for this selection (supplementary Fig S3 online). *E. coli* Δ*bamE* was complemented with a plasmid encoding full-length wild-type BamE (pBAME), restoring its ability to grow in the presence of vancomycin. Subsequently, plasmids encoding mutants of BamE with cysteine or glycine substitutions were used to identify key residues (Table 1; supplementary Fig S4 online), with expression levels verified by western blotting (supplementary Fig S5 online). We predicted that three classes of mutation would be produced; those affecting the structural integrity of BamE, those affecting function and those with no measurable effects. We hypothesized that mutants in which structural integrity was compromised would be degraded, resulting in diminished levels of BamE. By contrast, mutants in which function is affected would show stable expression levels but produce increased susceptibility to vancomycin. Mutagenesis revealed that one of the most essential BamE residues was Cys 20, which is consistent with its requirement for acylation and subsequent localization to the outer membrane (Narita *et al*, 2004; Sklar *et al*, 2007). As expected, proteins containing mutations in the hydrophobic core residues I46G, V55G, L59G, Y75G, L91G, L93G, F95G and L101G failed to complement Δ*bamE*, and levels of protein were diminished; however, substitution with a hydrophobic cysteine residue was generally not as debilitating (supplementary Fig S4,S5 online). Unlike the above mutants, proteins containing single point mutations at I32G, Q34G/C, G35C, N36G/C, Y37G, L38G, M64G/C, D66G, F68G/C, W73G, F74G, V76G, R78G and Q88C were stably expressed (supplementary Fig S5 online), but did not restore the barrier function of the outer membrane on complementation of Δ*bamE*. Several other mutations caused slight defects in barrier function (supplementary Fig S4 online). The amino acids predicted to be functionally relevant are highly conserved among BamE molecules (supplementary Fig S6 online) and predominantly map to a single surface area (Fig 1C), indicating that this region has a functional role.

As BamE localizes to the outer membrane inner leaflet (Ochsner *et al*, 1999), we explored its interactions with phosphatidylglycerol, phosphatidylethanolamine or cardiolipin-containing micelles by using NMR. Only dihexanoyl phosphatidylglycerol (DHPG) bound, inducing substantial $^{1}H,^{15}N$ chemical shift perturbations in 22% of BamE's amide resonances both above and below its critical micelle concentration, suggesting that it can bind to a bilayer or to a single lipid (Fig 3; supplementary Fig S7 online). The specific perturbations were mapped to an exposed site that overlaps with the amino acids identified as functionally important. Mutations of residues directly affected by phosphatidylglycerol binding and those within the vicinity (Y37A, L38A, T61A, L63A, D66A, F68A, T70A, N71A, F74A, Y75A, V76A, Y37A-L38A and T70A-N71A) were subjected to $^{1}H^{15}N$-heteronuclear single quantum coherence (HSQC) binding studies. Although several of the mutants (Y37A, T70A and Y75A) could not be expressed sufficiently, those that could were confirmed by NMR to be stably folded. Only F74A caused abolition of phosphatidylglycerol binding (Fig 3C; supplementary Fig S8 online). This residue is exposed and centrally located in the observed phosphatidylglycerol binding site; however, its perturbations could not be directly measured by NMR binding methods because of peak overlap. The results are consistent with functional mutagenesis, which showed abolition of BamE function on mutation to F74G (with no loss of expression). Interestingly, mutation of Thr 70 or Asn 71, the two residues most perturbed by PG binding, did not alter binding efficiency, nor did their mutation affect function. We suggest that the observed chemical shifts are the result of an indirect structural change occurring in the α2–β1 loop on phosphatidylglycerol binding, rather than because of a direct interaction.

To elucidate how BamE is incorporated into the Bam complex, individual Bam proteins were tested for their interactions by using

Table 1 | BamE mutations that affect *Escherichia coli* sensitivity to vancomycin

Mutation	Sensitivity to vancomycin (μg/ml)
WT	100
C20G[a]	10
I32G[a]	50
Q34G/C[a]	30/10
G35C[a]	10
N36G/C[a]	10/10
Y37G[a]	30
L38G[a]	30
I46G[b]	10
V55G[b]	10
L59G[b]	10
M64G/C[a]	10/50
D66G[a]	50
F68G/C[a]	50/50
W73G[a]	50
F74G[a,c]	10
Y75G/C[b]	10/10
V76G[a]	10
R78G[a]	30
Q88C[a]	30
L91G[b]	10
L93G[b]	30
F95G/C[b]	10/30
L101G[b]	10

Mutations showing significant increases in susceptibility to vancomycin ($\leqslant$50 μg/ml, at least half the concentration needed to block growth of the wild-type strain) are listed with their minimal inhibitory concentrations shown. In the case of both glycine and cysteine point mutations showing susceptibility, both minimal inhibitory concentrations are highlighted. Those residues in positions that are predicted to affect the [a]function or [b]the structural integrity of BamE are highlighted. Structurally critical mutations were identified by multiple techniques including NMR, structural inspection and by measuring levels of BamE within the cell, with those compromising structural integrity showing degradation, resulting in diminished levels of BamE. [c]Mutation of Phe 74 to alanine completely abolished DHPG binding. WT, wild type.

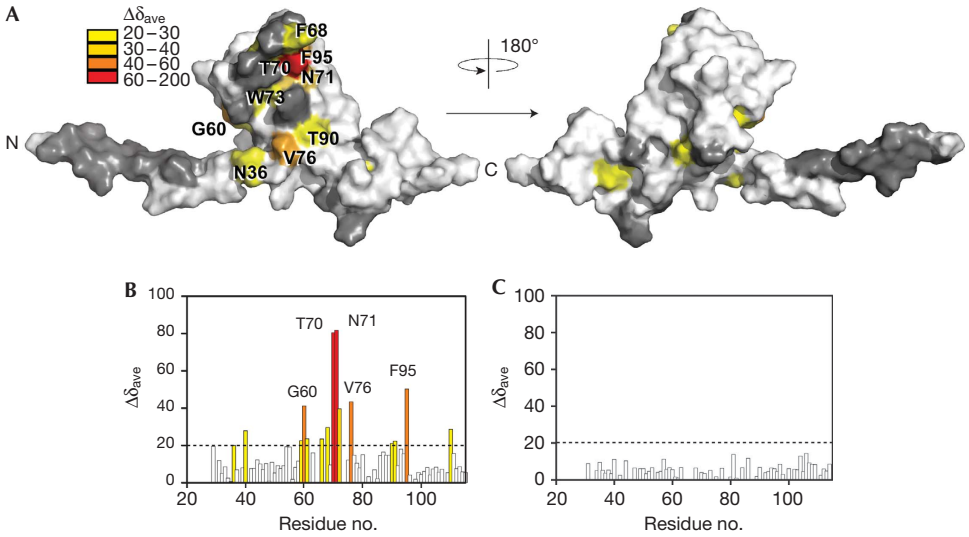

Fig 3 | BamE binds phosphatidylglycerol. (**A**) BamE surface representation highlighting residues showing degrees of substantial CS perturbations ($\Delta\delta_{ave}$ is the square root of $(((\Delta\delta_{HN}\times 500)^2 + \Delta\delta_N + 50.7)^2)$ on DHPG micelle interaction. (**B**) Histogram showing CS perturbations induced in ^{15}N-BamE (100 μM) on addition of DHPG (40 mM), coloured according to **A**. (**C**) Histogram showing the CS perturbations induced in labelled BamE (F74A; 100 μM) on addition of DHPG (40 mM). BamE, β-barrel assembly machine E; CS, chemical shift; DHPG, dihexanoyl phosphatidylglycerol.

NMR. Only BamD bound to BamE, consistent with previous studies (Sklar *et al*, 2007). Assembly of the BamE–BamD complex induced both line broadening and chemical shift perturbations at specific residues, showing slow exchange on the NMR timescale and defining an extensive interface consistent with strong binding (Fig 4). The surface circumscribed by the BamD interaction overlaps with the functionally crucial mutations and those involved in phosphatidylglycerol binding, although the profile of changes by each ligand is distinct. Importantly, the BamD site is larger and also includes Leu 63 and proximal residues Arg 29 and Ile 32 in the N-terminal disordered region. To test whether the determinants were distinct, we tested whether the F74A mutation, which abolishes DHPG binding, affects BamD interaction. The ^{15}N-F74A mutant retained BamD binding activity. Its ^{1}H-^{15}N backbone signals broadened similarly to those of the wild type on addition of twofold excess of BamD. It should be noted that, as the BamD interface is extensive, multiple point mutations would probably be required to obliterate binding. Indeed, individual point mutations in BamE, including L38A, L63A, D66A, F68A and N71A, did not abolish binding on the basis of NMR line broadening, although small but significant effects cannot be excluded. Several highly conserved residues are exposed in the BamD binding site, including those of the QGN motif and Pro 62, Asp 66 and Phe 68 in the α2–β1 loop (signal of Asp 66 could not be measured because of exchange effects), and thus might mediate conserved interactions in the Bam complex. Interestingly, the essential QGN motif does not show substantial perturbations on binding to BamD or phosphatidylglycerol, and we speculate that its functional relevance might rather involve correct positioning of the flanking Ile 32 and Leu 38 residues during BamD engagements.

The proximity of the BamD and phosphatidylglycerol binding sites to each other led us to attempt assembly of the ternary complex. Addition of BamD to the DHPG–^{15}N-BamE complex broadens the amide signals of the structured residues, indicating the formation of a large, slowly tumbling complex, although the perturbations associated with DHPG binding are clearly retained (supplementary Fig S9 online). Addition of DHPG to the equimolar BamD–^{15}N-BamE complex induces chemical shift changes that reflect those seen during formation of the binary DHPG–^{15}N-BamE complex, indicating a similar mode of interaction. Thus, both assembly routes converge on the same ternary complex, indicating that neither interface is exclusive and is consistent with additive interactions. Interestingly in the ternary complex, BamE preferentially binds to phosphatidylglycerol in the unimolecular rather to than micellar mode, suggesting that an equimolar ternary complex predominates.

In conclusion, natively folded BamE is a monomeric lipoprotein that specifically recognizes phosphatidylglycerol through its structural domain. We propose that BamE engages phosphatidylglycerol through a site centred at Phe 74 with N-terminal acylation bolstering membrane attachment. It is possible that BamE has a role in phosphatidylglycerol transport; however, this seems unlikely as the phosphatidylglycerol composition of the outer membrane was unaltered in *E. coli* Δ*bamE* strains (supplementary Fig S10 and supplementary Table S2 online). Alternatively, this interaction might represent a new functional characteristic of the Bam complex, anchoring the associated Bam subunits to phosphatidylglycerol-rich regions (Vanounou *et al*, 2003). Importantly, phosphatidylglycerol has been shown to aid the insertion of OMPs into synthetic membranes (Patel *et al*, 2009). Moreover, it might locally disrupt the membrane, aiding OMP penetration. Although the roles and structures of the remaining Bam subunits are still to be elucidated, the dual protein- and lipid-anchoring mechanism of BamE provides an insight into the OMP assembly process.

METHODS

Methods associated with supplementary figures are supplied as part of supplementary information.

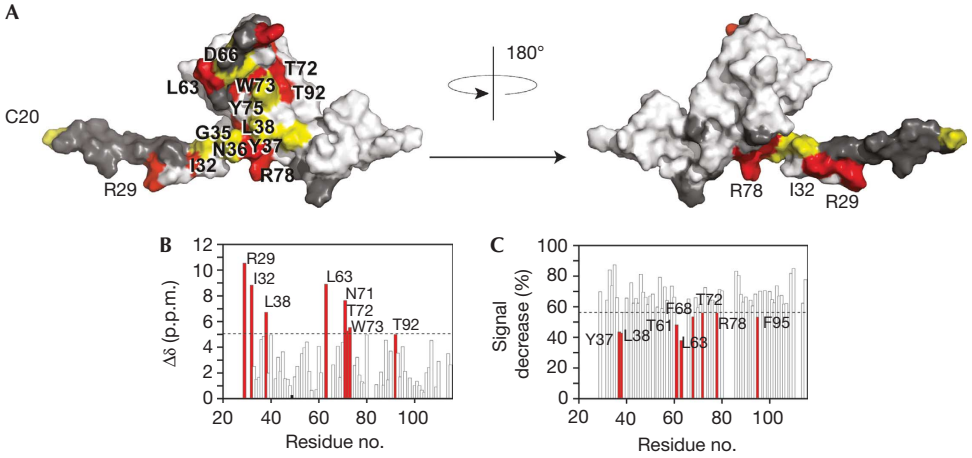

Fig 4 | The BamD binding site. (**A**) Surface representation of BamE. Residues shown by ^{1}H,^{15}N-resolved NMR that interact with BamD are shown in red, as estimated by showing either CS perturbations or specific line broadening. Residues shown by mutagenesis to be critical for function are shown in yellow. Residues in dark grey were either not assigned or not measured because of signal overlap. (**B**) Histogram showing normalized CS perturbations induced in ^{15}N-labelled BamE (70 μM) after addition of BamD (200 μM). (**C**) Histogram showing specific line broadening of ^{15}N-BamE residues (70 μM) on addition of BamD (200 μM). Residues larger than 1 s.d. from the mean (dashed line) were considered significant and are highlighted in red. Bam, β-barrel assembly machine; CS, chemical shift.

Cloning and protein purification. A detailed description of the cloning, expression and purification strategy is published elsewhere (Knowles *et al*, 2010); *E. coli* BamB, BamC and BamD were produced in the same manner (Knowles *et al*, 2009a).

NMR spectroscopy. Experiments were carried out at 298 K on a Varian Inova 800 MHz spectrometer equipped with a triple-resonance cryogenic probe and *z*-axis pulse-field gradients. The BamE concentration was 2 mM in 50 mM sodium phosphate (pH 7), 50 mM NaCl and 0.02% NaN_3 in 90% H_2O/10% D_2O. Spin system and sequential assignments were made from BEST CBCA(CO)NH, HNCACB, HNCA, HN(CO)CA, HNCO, HN(CA)-CO, H(C)CH TOCSY and (H)CCH TOCSY experiments (Schanda *et al*, 2006; Lescop *et al*, 2007). Spectra were processed with NMRPipe (Delaglio *et al*, 1995) and analysed with SPARKY (Goddard & Kneller, 2004).

Structure calculation. Proton distance restraints were obtained from ^{15}N- and ^{13}C-edited NOESY-HSQC spectra ($\tau_{mix} = 100$ ms). Backbone dihedral angle restraints (φ and ψ) were obtained using TALOS (Cornilescu *et al*, 1999). The structure was calculated iteratively using CANDID/CYANA, with automated NOE cross-peak assignment and torsion angle dynamics implemented (Guntert, 2004). A total of 20 conformers with the lowest CYANA target function were produced and they satisfied all measured restraints. Aria1.2 was used to perform the final water minimization (Linge *et al*, 2001). Structures were analysed using PROCHECK-NMR (Laskowski *et al*, 1993) and MOLMOL (Koradi *et al*, 1996). Structural statistics are summarized in supplementary Table S1 online.

Lipid interactions. Binding to 70 μM ^{15}N-BamE in 50 mM sodium phosphate (pH 7), 50 mM NaCl and 0.02% NaN_3 in 90% H_2O/10% D_2O was monitored by $^{1}H^{15}N$-HSQCs at concentrations of 0–50 mM of either DHPG (critical micelle concentration (c.m.c.), about 20 mM; Tan & Roberts, 1996) or DHPE (c.m.c., about 7 mM; Hergenrother & Martin, 1997). Cardiolipin titrations were performed in the presence of DHPE to enable solubilization, with DHPE/cardiolipin concentrations of 0/0, 6/0.6, 12/1.2, 18/18, 24/2.4 mM added.

Bam protein interactions. Binding of ^{15}N-BamE (70 μM) with unlabelled BamB, BamC and BamD proteins was performed by $^{1}H^{15}N$-HSQC titration experiments at concentrations of 0–500 μM unlabelled Bam accessory factors. Peak analysis was performed with CCPNMR (Vranken *et al*, 2005). The buffer used throughout was 50 mM sodium phosphate (pH 7), 50 mM NaCl and 0.02% NaN_3 in 90% H_2O/10% D_2O.

Construction of mutants. Wild-type *bamE* coding sequence was amplified from *E. coli* K-12 and cloned into pET20b (Novagen) to create pBAME. Single point cysteine/glycine mutagenesis was performed by using PCR with the primers described in supplementary Table S3 online, and the products were cloned into pBAME as appropriate. All constructs were confirmed by DNA sequencing.

Accession codes. Coordinates and NMR assignments have been deposited with accession codes 2km7 (PDB) and 16424 (BMRB), respectively.

Supplementary information is available at EMBO *reports* online (http://www.emboreports.org).

ACKNOWLEDGEMENTS

We thank S. Whittaker for NMR acquisitions and discussions, J. James for performing lipid extractions, L. Bishop for assistance with Fourier transform ion cyclotron resonance mass spectrometry processing, S. Galsinh for outer membrane preparations, L. Robinson for confirming Biolog phenotypes and the Henry Wellcome Building for Biomolecular NMR Spectroscopy. This research was funded by the Biotechnology and Biological Sciences Research Council (T.J.K., I.R.H. and M.O.), Medical Research Council (D.F.B., M.O. and I.R.H.) and EU PRISM projects.

CONFLICT OF INTEREST

The authors declare that they have no conflict of interest.

REFERENCES

Bos MP, Robert V, Tommassen J (2007) Biogenesis of the gram-negative bacterial outer membrane. *Annu Rev Microbiol* **61:** 191–214

Cornilescu G, Delaglio F, Bax A (1999) Protein backbone angle restraints from searching a database for chemical shift and sequence homology. *J Biomol NMR* **13:** 289–302

Delaglio F, Grzesiek S, Vuister GW, Zhu G, Pfeifer J, Bax A (1995) NMRPipe: a multidimensional spectral processing system based on UNIX pipes. *J Biomol NMR* **6:** 277–293

Gatsos X, Perry AJ, Anwari K, Dolezal P, Wolynec PP, Likic VA, Purcell AW, Buchanan SK, Lithgow T (2008) Protein secretion and outer membrane assembly in Alphaproteobacteria. *FEMS Microbiol Rev* **32:** 995–1009

Goddard TD, Kneller DG (2004) *SPARKY 3*. San Francisco, CA, USA: University of California

Guntert P (2004) Automated NMR structure calculation with CYANA. *Methods Mol Biol* **278:** 353–378

Hagan CL, Kim S, Kahne D (2010) Reconstitution of outer membrane protein assembly from purified components. *Science* **328:** 890–892

Hergenrother PJ, Martin SF (1997) Determination of the kinetic parameters for phospholipase C (*Bacillus cereus*) on different phospholipid substrates using a chromogenic assay based on the quantitation of inorganic phosphate. *Anal Biochem* **251:** 45–49

Holm L, Park J (2000) DaliLite workbench for protein structure comparison. *Bioinformatics* **16:** 566–567

Kim S, Malinverni JC, Sliz P, Silhavy TJ, Harrison SC, Kahne D (2007) Structure and function of an essential component of the outer membrane protein assembly machine. *Science* **317:** 961–964

Knowles TJ, Jeeves M, Bobat S, Dancea F, McClelland D, Palmer T, Overduin M, Henderson IR (2008) Fold and function of polypeptide transport-associated domains responsible for delivering unfolded proteins to membranes. *Mol Microbiol* **68:** 1216–1227

Knowles TJ, McClelland DM, Rajesh S, Henderson IR, Overduin M (2009a) Secondary structure and (1)H, (13)C and (15)N backbone resonance assignments of BamC, a component of the outer membrane protein assembly machinery in *Escherichia coli*. *Biomol NMR Assign* **3:** 203–206

Knowles TJ, Scott-Tucker A, Overduin M, Henderson IR (2009b) Membrane protein architects: the role of the BAM complex in outer membrane protein assembly. *Nat Rev Microbiol* **7:** 206–214

Knowles TJ, Sridhar P, Rajesh S, Manoli E, Overduin M, Henderson IR (2010) Secondary structure and (1)H, (13)C and (15)N resonance assignments of BamE, a component of the outer membrane protein assembly machinery in *Escherichia coli*. *Biomol NMR Assign* **4:** 179–181

Koradi R, Billeter M, Wuthrich K (1996) MOLMOL: a program for display and analysis of macromolecular structures. *J Mol Graph* **14:** 51–55, 29–32

Laskowski RA, MacArthur MW, Moss DS, Thornton JM (1993) PROCHECK: a program to check the stereochemical quality of protein structures. *J Appl Crystallogr* **26:** 283–291

Lescop E, Schanda P, Brutscher B (2007) A set of BEST triple-resonance experiments for time-optimized protein resonance assignment. *J Magn Reson* **187:** 163–169

Linge JP, O'Donoghue SI, Nilges M (2001) Automated assignment of ambiguous nuclear overhauser effects with ARIA. *Methods Enzymol* **339:** 71–90

Malinverni JC, Werner J, Kim S, Sklar JG, Kahne D, Misra R, Silhavy TJ (2006) YfiO stabilizes the YaeT complex and is essential for outer membrane protein assembly in *Escherichia coli*. *Mol Microbiol* **61:** 151–164

Narita S, Matsuyama S, Tokuda H (2004) Lipoprotein trafficking in *Escherichia coli*. *Arch Microbiol* **182:** 1–6

Ochsner UA, Vasil AI, Johnson Z, Vasil ML (1999) *Pseudomonas aeruginosa* fur overlaps with a gene encoding a novel outer membrane lipoprotein, OmlA. *J Bacteriol* **181:** 1099–1109

Patel GJ, Behrens-Kneip S, Holst O, Kleinschmidt JH (2009) The periplasmic chaperone Skp facilitates targeting, insertion, and folding of OmpA into lipid membranes with a negative membrane surface potential. *Biochemistry* **48:** 10235–10245

Ruiz N, Falcone B, Kahne D, Silhavy TJ (2005) Chemical conditionality: a genetic strategy to probe organelle assembly. *Cell* **121:** 307–317

Schanda P, Van Melckebeke H, Brutscher B (2006) Speeding up three-dimensional protein NMR experiments to a few minutes. *J Am Chem Soc* **128:** 9042–9043

Sklar JG, Wu T, Gronenberg LS, Malinverni JC, Kahne D, Silhavy TJ (2007) Lipoprotein SmpA is a component of the YaeT complex that assembles outer membrane proteins in *Escherichia coli*. *Proc Natl Acad Sci USA* **104:** 6400–6405

Tan CA, Roberts MF (1996) Vanadate is a potent competitive inhibitor of phospholipase C from *Bacillus cereus*. *Biochim Biophys Acta* **1298:** 58–68

Vanini MM, Spisni A, Sforca ML, Pertinhez TA, Benedetti CE (2008) The solution structure of the outer membrane lipoprotein OmlA from *Xanthomonas axonopodis* pv. *citri* reveals a protein fold implicated in protein–protein interaction. *Proteins* **71:** 2051–2064

Vanounou S, Parola AH, Fishov I (2003) Phosphatidylethanolamine and phosphatidylglycerol are segregated into different domains in bacterial membrane. A study with pyrene-labelled phospholipids. *Mol Microbiol* **49:** 1067–1079

Voulhoux R, Bos MP, Geurtsen J, Mols M, Tommassen J (2003) Role of a highly conserved bacterial protein in outer membrane protein assembly. *Science* **299:** 262–265

Vranken WF, Boucher W, Stevens TJ, Fogh RH, Pajon A, Llinas M, Ulrich EL, Markley JL, Ionides J, Laue ED (2005) The CCPN data model for NMR spectroscopy: development of a software pipeline. *Proteins* **59:** 687–696

Vuong P, Bennion D, Mantei J, Frost D, Misra R (2008) Analysis of YfgL and YaeT interactions through bioinformatics, mutagenesis, and biochemistry. *J Bacteriol* **190:** 1507–1517

Wu T, Malinverni J, Ruiz N, Kim S, Silhavy TJ, Kahne D (2005) Identification of a multicomponent complex required for outer membrane biogenesis in *Escherichia coli*. *Cell* **121:** 235–245